



Dielectric tunability properties of the $\text{Pb}[(\text{Mg}_{1/3}\text{Nb}_{2/3})_{1-x}\text{Zr}_x]\text{O}_3$ ceramics

Biaolin Peng^a, Huiqing Fan^{a,*}, Qiang Li^a, Qi Zhang^b

^a State Key Laboratory of Solidification Processing, School of Materials Science and Engineering, Northwestern Polytechnical University, Xi'an 710072, China

^b Department of Manufacturing and Materials, Cranfield University, Cranfield, Bedfordshire MK43 0AL, United Kingdom

ARTICLE INFO

Article history:

Received 24 July 2012

Received in revised form 17 August 2012

Accepted 2 September 2012

Available online 28 September 2012

Keywords:

$\text{Pb}[(\text{Mg}_{1/3}\text{Nb}_{2/3})_{1-x}\text{Zr}_x]\text{O}_3$ ceramics

Relaxor ferroelectrics

Dielectric tunability

Nanopolar clusters

ABSTRACT

$\text{Pb}[(\text{Mg}_{1/3}\text{Nb}_{2/3})_{1-x}\text{Zr}_x]\text{O}_3$ ($x = 0.03, 0.06, 0.09, 0.12$) ceramics were prepared using a solid state reaction process. The phase structure and surface micrograph were analyzed by X-ray diffraction and scanning electron microscopy. The effects of Zr content on the dielectric and dielectric tunability properties were investigated systematically. The results showed that the high dielectric tunability ($>75\%$ at $x = 0.12$), low dielectric loss ($<0.15\%$) and high temperature stability of these relaxor ferroelectric ceramics were favorable and competitive to those of titanium-containing perovskite structure materials for tunable device applications. The high dielectric non-linear properties were further discussed in terms of the Landau–Ginsberg–Devonshire thermodynamic theory completed with a Langevin term.

© 2012 Elsevier B.V. All rights reserved.

1. Introduction

With the rapid development of tunable devices, non-linear dielectric materials with higher tunability and lower dielectric loss have been investigated extensively. Among the numerous perovskite structure materials that exhibit variable permittivity under an external dc bias field, $(\text{Ba},\text{Sr})\text{TiO}_3$ (BST), $\text{Ba}(\text{Zr},\text{Ti})\text{O}_3$ (BZT) and $(\text{Pb},\text{Sr})\text{TiO}_3$ (PST) were regarded as the most suitable candidates for electronically tunable components [1–4].

However, the oxidation state of titanium was easily reduced from Ti^{4+} to Ti^{3+} at a higher temperature [5]. Accordingly, the dielectric properties of titanium-containing (BST, BZT, PST, etc.) usually undergo degradation (dielectric loss increasing) at a higher temperature and a higher external electric field. To improve the dielectric properties of these materials for tunable applications, many efforts have been made by, for example, the element doping. It is well known that a small amount of acceptor dopants can dramatically modify the dielectric properties. Some dopants, like Mn^{2+} , Mn^{3+} , Fe^{2+} , Fe^{3+} , Co^{2+} , Co^{3+} , Ni^{2+} , etc. [6–12], can occupy the B sites of the (ABO_3) perovskite structure and behave as electron acceptors. They have been known to lower dielectric loss. Another effective way is to dope the oxides that have low dielectric losses, such as MgO , Al_2O_3 , MgAl_2O_4 , etc., into the dielectric materials as the second phase existing [13–15]. However, the dielectric permittivity and tunability were also decreased simultaneously as the dielectric loss was decreased. Therefore, looking for new tunable perovskite materials that do not contain titanium ions may

provide a feasible way to obtain low dielectric loss while keeping a high tunability.

In this work, the dielectric tunability properties of $\text{Pb}[(\text{Mg}_{1/3}\text{Nb}_{2/3})_{1-x}\text{Zr}_x]\text{O}_3$ relaxor ferroelectric ceramics were investigated. The observed dielectric non-linearity is modeled with the Landau–Ginsberg–Devonshire thermodynamic theory plus a Langevin term that describes the contribution of the re-orientation of the polar nanoclusters to the non-linear $\epsilon(E)$ dependences.

2. Experimental procedure

$\text{Pb}[(\text{Mg}_{1/3}\text{Nb}_{2/3})_{1-x}\text{Zr}_x]\text{O}_3$ ($x = 0.03, 0.06, 0.09, 0.12$) ceramics were prepared by solid-state reactions [16,17]. MgO and Nb_2O_5 powders were pre-reacted at 1100°C for 6 h in air to form MgNb_2O_6 and then the formed MgNb_2O_6 powders were mixed with stoichiometric amounts of PbO and ZrO_2 and calcined at 900°C for 2 h. Pressed pellets with a diameter of 10 mm and thickness of 1 mm, were formed by cold-isostatic pressing at 300 MPa. The preformed pellets were sintered at 1240°C for 2 h and then cooled naturally to room temperature. Sintering was carried out inside a covered alumina crucible, and the pellets were covered with powder of the same composition to minimize the loss of lead during firing.

The crystal structures of the sintered pellets were analyzed using X-ray diffraction (XRD; D/Max2550VB+/PC, Rigaku, Tokyo, Japan) with Cu K_α radiation ($\lambda = 0.15406\text{ nm}$) over 2θ in the range of 10° – 60° . The crystal phases were compared with the powder diffraction data from JCPDS-ICDD (International Center of Diffraction Data). The density of all the pellets was measured by the Archimedes method. The microstructure of the sintered pellets was investigated using a scanning electron microscopy with an applied voltage of 20 kV (SEM; Model JEOL-6700F, Japan Electron Co., Tokyo, Japan).

For the electrical property measurements, silver paste was painted on the polished pellets as the electrodes and fired at 550°C for 30 min. Weak-field dielectric response at a signal level of 500 mV/mm were measured by using a precision impedance analyzer (4294A, Agilent, CA, USA) associated with temperature controller (TP94, Linkam, Surrey, UK) at a heating rate of $3^\circ\text{C}/\text{min}$. The depolarization current density was measured with a High Resistance Meter (4339B, Agilent, CA, USA).

* Corresponding author. Tel.: +86 29 88494463; fax: +86 29 88492642.

E-mail address: hqfan3@163.com (H. Fan).

Before the measurement, all samples were cooled from room temperature down to lower temperature under an electric field of 10 kV/cm. The dc bias electric field dependence of the dielectric permittivity was measured at 10 kHz and 300 K.

3. Results and discussions

3.1. Structure and electrical property

Fig. 1 shows the XRD patterns of sintered $\text{Pb}[(\text{Mg}_{1/3}\text{Nb}_{2/3})_{1-x}\text{Zr}_x]\text{O}_3$ ($x = 0.03, 0.06, 0.09, 0.12$) ceramics. Only single perovskite phase can be detected at all compositions, with no traces from other impurity phases (pyrochlore phases, etc.), indicating that a solid solution has been formed. With increasing Zr contents, the (100) peak slightly shifts to lower diffraction angle, implying an increased scale in the cell parameter (a).

Fig. 2 gives the SEM micrographs of $\text{Pb}[(\text{Mg}_{1/3}\text{Nb}_{2/3})_{1-x}\text{Zr}_x]\text{O}_3$ ($x = 0.03, 0.06, 0.09, 0.12$) ceramics. All sample show dense microstructure, meanwhile density measurements also reveal that all samples have relative densities in the range of 95%–98%. With the increase of Zr content, the average grain size of $\text{Pb}[(\text{Mg}_{1/3}\text{Nb}_{2/3})_{1-x}\text{Zr}_x]\text{O}_3$ ceramics decreases from 5 μm at $x = 0.03$ to 3 μm at $x = 0.12$, indicating that Zr-doping has a significant effect on the grain size of $\text{Pb}[(\text{Mg}_{1/3}\text{Nb}_{2/3})_{1-x}\text{Zr}_x]\text{O}_3$ ceramics.

The temperature dependences of the dielectric permittivity ($\varepsilon(T)$) of $\text{Pb}[(\text{Mg}_{1/3}\text{Nb}_{2/3})_{1-x}\text{Zr}_x]\text{O}_3$ ($x = 0.03, 0.06, 0.09, 0.12$) ceramics at 10 kHz are shown in Fig. 3a. As the Zr content increases, the temperature at the $\varepsilon(T)$ maximum, T_m , increases from 275 K at $x = 0.03$ to 297 K at $x = 0.12$ and the corresponding dielectric permittivity value increases from 12884 to 15946. Also, the dielectric permittivity value at 300 K increases from 10344 to 15727. According to the neutron diffuse scattering data of the pure PMN relaxor ferroelectric [18], upon cooling the number of polar nanoregions (PNRs) first increases and then, at lower temperatures, decreases. As a result, the T_m appears. Therefore, it can be understood that the relative amount of PNRs in $\text{Pb}[(\text{Mg}_{1/3}\text{Nb}_{2/3})_{1-x}\text{Zr}_x]\text{O}_3$ ($x = 0.03, 0.06, 0.09, 0.12$) ceramics at the paraelectric state ($T > T_m$) increases with increasing Zr content.

In order to describe the dielectric relaxor behavior at $T > T_m$, several relations have been proposed such as the Vogel–Fulcher (V–F) relation, the modified Curie–Weiss relation, the Lorentz-type empirical relation [19,20], etc. Among these relations, the most effective one is the Lorentz-type empirical relation,

$$\varepsilon_A/\varepsilon = 1 + (T - T_A)^2/2\delta_A^2 \quad (1)$$

where T_A ($T_A \neq T_m$) and ε_A are the temperature of the dielectric peak and the extrapolated value of ε at $T = T_A$, respectively. The param-

eter δ_A is temperature and frequency independent, reflecting the relaxor diffuseness of the dielectric peak. The greater the relaxor dispersion is, the bigger δ_A is. Furthermore, it is found that Eq. (1) not only can describe the high temperature ($T > T_m$) dielectric permittivity quite well in a number of relaxor ferroelectrics [19,20], but also can do in the normal ferroelectrics such as the BaTiO_3 [21,22]. Likewise at $T > T_m$, the $\varepsilon'(T)$ of the $\text{Pb}[(\text{Mg}_{1/3}\text{Nb}_{2/3})_{1-x}\text{Zr}_x]\text{O}_3$ ($x = 0.03, 0.06, 0.09, 0.12$) ceramics can well be fitted by the Eq. (1) (see the black short dash dot lines in Fig. 3a). Accordingly, the best Lorentz fitting parameters are listed in Table 1. It can be seen that the δ_A decreases from 106 at $x = 0.03$ to 96 at $x = 0.12$, indicating that a decreasing degree of the relaxor dispersion is accompanied with increasing Zr content.

Fig. 3b shows the temperature dependence of the thermal depolarization current ($J(T)$) of $\text{Pb}[(\text{Mg}_{1/3}\text{Nb}_{2/3})_{1-x}\text{Zr}_x]\text{O}_3$ ($x = 0.03, 0.06, 0.09, 0.12$) ceramics. The measured parameters are also listed in Table 1. With increasing Zr content, the thermal depolarization temperature (T_{d0}) increases from 182 K at $x = 0.03$ to 233 K at $x = 0.12$, and the thermal depolarization current maximum (J_m) increases from 0.39 mA/m² at $x = 0.03$ to 0.79 mA/m² at $x = 0.12$. Only a weak and broad current peak was detected for $x = 0.03$ during heating, in contrast, with increasing Zr content, stronger and narrower peaks were detected, indicating that the thermal depolarization process in high Zr content occurred in a relatively narrow temperature range. It has been well documented that the gap between $T_m - T_{d0}$ reflects the degree of the electric dipole order in relaxor ferroelectrics ceramics [23]. The smaller $T_m - T_{d0}$ is, the bigger the degree of the electric dipole order is. In Table 1, it can be seen that $T_m - T_{d0}$ value decreases from 91 K at $x = 0.03$ to 61 K at $x = 0.12$, indicating that an increasing electric dipole order is accompanied with increasing Zr content. In addition, the high J_m value and its increase with increasing Zr content also imply that large pyroelectric and/or electrocaloric effect at room temperature can be obtained at higher Zr content.

Fig. 3c exhibits the temperature dependence of the dielectric loss ($\tan \delta(T)$) of $\text{Pb}[(\text{Mg}_{1/3}\text{Nb}_{2/3})_{1-x}\text{Zr}_x]\text{O}_3$ ($x = 0.03, 0.06, 0.09, 0.12$) ceramics at 10 kHz. With increasing Zr content, the temperature of the $\tan \delta(T)$ maximum ($T_{m\delta}$) shifts to higher temperature from 245 K at $x = 0.03$ to 271 K at $x = 0.12$, and the dielectric loss value at 300 K increases from 0.003 at $x = 0.03$ to 0.013 at $x = 0.12$. The dielectric loss of all ceramics is acceptable for tunable application (<2%). Furthermore, the dielectric losses of $\text{Pb}[(\text{Mg}_{1/3}\text{Nb}_{2/3})_{1-x}\text{Zr}_x]\text{O}_3$ ceramics all remain low and stable (<0.3%) in a wide temperature range (325–450 K), indicating that the abilities of undergoing degradation (dielectric loss increasing) at a higher temperature are very strong. In contrast, the abilities of undergoing degradation for titanium-containing ceramics, such as the $\text{Ba}_{60}\text{Sr}_{40}\text{TiO}_3$ (see the inset of Fig. 3c), are not favorable for tunable applications.

Fig. 3d illustrates the dc bias electric field dependence of the dielectric tunability ($n_r(E)$) of $\text{Pb}[(\text{Mg}_{1/3}\text{Nb}_{2/3})_{1-x}\text{Zr}_x]\text{O}_3$ ($x = 0.03, 0.06, 0.09, 0.12$) ceramics at 300 K and 10 kHz. The dielectric tunability (n_r) was calculated by using the expression [24,25].

$$n_r = (\varepsilon(0) - \varepsilon(E))/\varepsilon(0) \quad (2)$$

where $\varepsilon(0)$ and $\varepsilon(E)$ represent the dielectric permittivity at zero and a certain electric field, respectively. With the increase of Zr content, n_r increases from 0.62 at $x = 0.03$ to 0.75 at $x = 0.12$ at 25 kV/cm. These values are competitive to titanium-containing dielectric ceramics ($\text{BaZr}_{0.30}\text{Ti}_{0.70}\text{O}_3$, $n_r = 0.45$ and $\tan \delta = 0.002$ at 40 kV/cm; $\text{Pb}_{0.35}\text{Sr}_{0.65}\text{TiO}_3$, $n_r = 0.48$ and $\tan \delta = 0.008$ at 40 kV/cm [25,26], etc.). Furthermore, the high tunability value leaves more rooms for further decreasing the dielectric loss by adding additives with low dielectric losses such as MgO , Al_2O_3 , MgAl_2O_4 , etc.

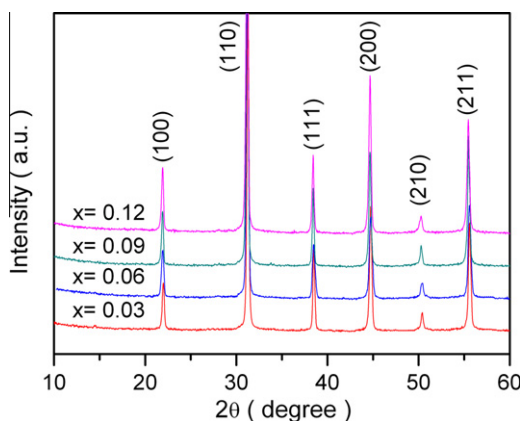


Fig. 1. XRD patterns of $\text{Pb}[(\text{Mg}_{1/3}\text{Nb}_{2/3})_{1-x}\text{Zr}_x]\text{O}_3$ ceramics.

Download English Version:

<https://daneshyari.com/en/article/1615179>

Download Persian Version:

<https://daneshyari.com/article/1615179>

[Daneshyari.com](https://daneshyari.com)